

Cathodoluminescence versus dynamical epitaxy of Ba²⁺-ion irradiated α -quartz

S. Dhar, S. Gašiorek, P. K. Sahoo, U. Vetter, H. Hofstätter, V. N. Kulkarni, and K. P. Lieb

Citation: *Applied Physics Letters* **85**, 1341 (2004); doi: 10.1063/1.1784538

View online: <http://dx.doi.org/10.1063/1.1784538>

View Table of Contents: <http://scitation.aip.org/content/aip/journal/apl/85/8?ver=pdfcov>

Published by the [AIP Publishing](#)

Articles you may be interested in

[Light-emitting defects and epitaxy in alkali-ion-implanted \$\alpha\$ quartz](#)

Appl. Phys. Lett. **88**, 261102 (2006); 10.1063/1.2215615

[Cathodoluminescence and solid phase epitaxy in Ba²⁺-irradiated \$\alpha\$ -quartz](#)

J. Appl. Phys. **97**, 014910 (2005); 10.1063/1.1829791

[Stable violet cathodoluminescence of \$\alpha\$ -quartz after Ge²⁺ implantation at elevated temperature](#)

J. Appl. Phys. **96**, 1392 (2004); 10.1063/1.1767973

[Chemically guided epitaxy of Rb-irradiated \$\alpha\$ -quartz](#)

J. Appl. Phys. **95**, 4705 (2004); 10.1063/1.1689733

[Ion-beam induced amorphization and dynamic epitaxial recrystallization in \$\alpha\$ -quartz](#)

J. Appl. Phys. **85**, 3120 (1999); 10.1063/1.369650

An advertisement for KeySight B2980A Series Picoammeters/Electrometers. The ad features a red banner with white text that reads 'Confidently measure down to 0.01 fA and up to 10 PΩ'. Below this, it says 'KeySight B2980A Series Picoammeters/Electrometers' and includes a 'View video demo' button. To the right of the text is an image of the device, and to the far right is the KeySight Technologies logo.

Cathodoluminescence versus dynamical epitaxy of Ba-ion irradiated α -quartz

S. Dhar,^{a)} S. Gašiorek,^{b)} P. K. Sahoo,^{c)} U. Vetter, H. Hofsäß, V. N. Kulkarni,^{c)} and K. P. Lieb^{d)}

II. Physikalisches Institut, Universität Göttingen, Tammannstraße 1, D-37077 Göttingen, Germany

(Received 14 January 2004; accepted 18 June 2004)

Doping α -quartz with photoactive ions without destroying its crystalline structure appears to be a promising way to tune its luminescent and structural properties. We have achieved dynamic solid phase epitaxial regrowth and cathodoluminescence of 175 keV Ba-ion irradiated α -quartz in the temperature range from 300 to 1170 K. Rutherford Backscattering Channeling analysis showed that the amorphous layer produced by 1×10^{15} Ba ions/cm² at 300 K had almost disappeared at an implantation temperature of 1123 K. Room temperature cathodoluminescence exhibited dramatic changes in the optical spectra as a function of the implantation temperature and allowed to distinguish between color centers related to quartz, ion-irradiated silica and implanted Ba. Between 770 and 1100 K, room-temperature cathodoluminescence showed a predominant blue and other weak bands connected to various known defects in the $\equiv\text{Si-O-Si}\equiv$ network. However, after achieving almost complete solid phase epitaxial recovery, only a violet band at 3.4 eV remained, which we attribute to Ba-related luminescence centers. © 2004 American Institute of Physics.

[DOI: 10.1063/1.1784538]

Due to its high chemical and thermal stability, amorphous and crystalline silicon dioxide (α -SiO₂, silica, c -SiO₂, quartz), a wide-band gap material, is extensively used in fabricating various optoelectronic and photonic devices such as optical waveguides, resonators, switches, and splitters.¹⁻³ Due to its high technological importance, various fundamental properties have been studied.⁴⁻⁷ Major efforts are also undertaken to construct light-emitting devices by doping SiO₂ with semiconducting and metal elements using various processing techniques.^{3,8-13} For example, strong blue and violet photoluminescence has been reported after Ge-ion implantation into α -SiO₂ and vacuum annealing.^{8,10,13} Both pure amorphous and crystalline SiO₂ show weak intrinsic luminescence light in the visible range. The luminescent properties and associated centers are very sensitive to the preparation methods of the samples, depending on intrinsic and radiation-induced defects, flexibility of the SiO₂ network structure, microstructure of the implanted species, mechanical stress, temperature treatment, and many other factors.^{3,14-19}

Many of these problems could be avoided by introducing the dopants directly into the quartz matrix without destroying its crystalline structure. For instance, the formation of small Si or Ge clusters or nanocrystals embedded in α -quartz would be possible and may offer attractive optical applications in future. However, because of its structural constraints, quartz gets easily amorphized during implantation of the dopants at low temperature. The critical energy density E_c ,

which needs to be deposited to achieve amorphization is given by $E_c = \Phi_c F_D^{\max}$, where Φ_c is the critical fluence for amorphization and F_D^{\max} is the maximum deposited energy, which depends on the energy and mass of the incident ions and target atoms.²⁰⁻²³ The attempts to achieve complete solid phase epitaxial regrowth (SPEG) of such amorphous layers via thermal vacuum postannealing have not been successful. Only recently, we developed two methods to achieve complete SPEG of ion irradiated synthetic α -quartz (or thin α -SiO₂ films on quartz): (1) in dynamical SPEG,²¹ the Ne ions are implanted in vacuum into the heated α -quartz in such a fashion that the radiation damages are removed during the implantation process itself and crystalline quartz is restored; (2) in chemically guided SPEG,²⁴⁻²⁷ quartz is irradiated with alkali ions and then postannealed in oxygen or in air. While the alkali ions diffuse out of the sample, this process can also lead to full epitaxy.

In the present letter we report almost complete dynamic epitaxy of α -quartz during Ba ion implantation. In contrast to previous studies of epitaxy after irradiation with noble gas and alkali ions, which diffuse out during the respective thermal treatments, the implanted species (Ba) remain in the matrix during the recrystallization process. By measuring the cathodoluminescence (CL) spectra during the epitaxy, we demonstrate that the luminescence properties are highly correlated to the structural transformations of the matrix during implantations in the temperature range between 300 and 1170 K. This provides the possibility to distinguish between various color centers (related to either quartz or ion-beam amorphized silica or the implanted Ba ions themselves). Besides achieving epitaxy after the implantation of optical dopants, this work adds to answering the fundamental questions of the origin and thermal behavior of luminescence centers in SiO₂.

Polished α -quartz samples, (0001) oriented were irradiated with 175 keV (and 800 keV) Ba⁺ ions (beam current $\sim 0.5 \mu\text{A}$) to a fixed fluence of $1 \times 10^{15}/\text{cm}^2$ at temperatures

^{a)} Author to whom correspondence should be addressed; present address: Center for Superconductivity Research, Dept. of Physics, University of Maryland, College Park, MD 20742; electronic mail: dhar@squid.umd.edu.

^{b)} Also at: Henryk Niewodniczanski Institute of Nuclear Physics, ul. Radzikowskiego 152, PL-31342 Kraków, Poland.

^{c)} Permanent address: Department of Physics, Indian Institute of Technology Kanpur, Kanpur-208016, India.

^{d)} Electronic mail: plieb@gwdg.de

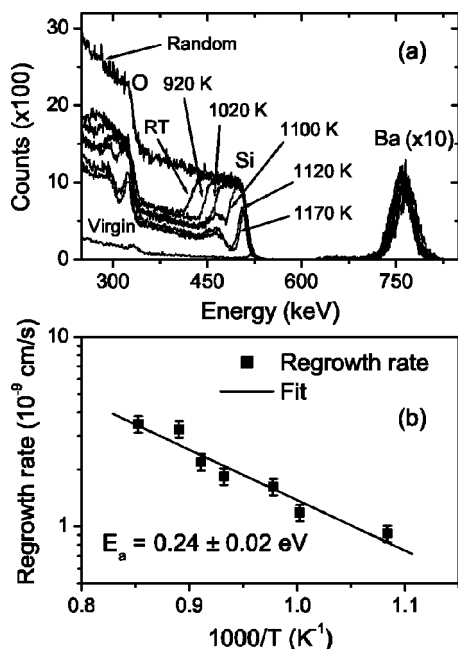


FIG. 1. (a) RBS-channeling spectra showing dynamic SPEG of the SiO_2 matrix for increasing sample temperature during 175 keV Ba^+ ions implantation at a fluence of 1×10^{15} ions/cm². The channeling and random spectra of a nonirradiated sample are also given. (b) Regrowth speed of Ba-doped quartz as a function of sample temperature.

between 300 and 1170 K. The damage and Ba depth distributions were monitored by means of Rutherford backscattering-channeling (RBS-C) with a 0.9 MeV α -beam obtained from Göttingen ion implanter IONAS. The RBS data were analyzed with the program RUMP²⁸ and DAMAGE.²⁰ CL measurements were performed using a 5 keV, 2 μA (1 W/cm²) e-beam (specs EQ-22) in the temperature range from 12 K to room-temperature (RT), using a closed-cycle helium refrigerator. The luminescence light was detected by a Hamamatsu R928 photomultiplier after focusing into a Czerny-Turner spectrograph (Jobin Yvon 1000M). CL spectra from different spots on the samples were collected for 700 s (speed 1 nm/s) in the wavelength range from 200 to 900 nm.

First we present the results on the dynamic epitaxy of α -quartz after 175 keV Ba^+ implantation as function of the sample temperature [see Fig. 1(a)]. After Ba implantation at RT, the height of the RBS signals from both the Si and the O sublattice in the near-surface region reached the random level indicating the formation of a 175-nm-thick homogeneous amorphous layer. For increasing sample temperature, the thickness of the amorphous layer decreased indicating a gradual and planar recrystallization process. Above 1100 K, radiation-induced damage and dynamic thermal recrystallization compensated each other and hence (almost) no damage remained in the sample for this fluence. The Ba profiles in all the cases were Gaussian-shaped; the measured average projected range of 75 nm compares rather well with the value 64 nm, calculated with the program SRIM.²⁹ It may be noted that SPEG (figure is not shown here) did not occur after Ba implantation at liquid nitrogen temperature followed by vacuum annealing up to 1370 K. From the damage profiles, the regrowth speed of the epitaxially recovered layers was determined as a function of temperature and is plotted in Fig. 1(b). It shows Arrhenius behavior with an activation energy

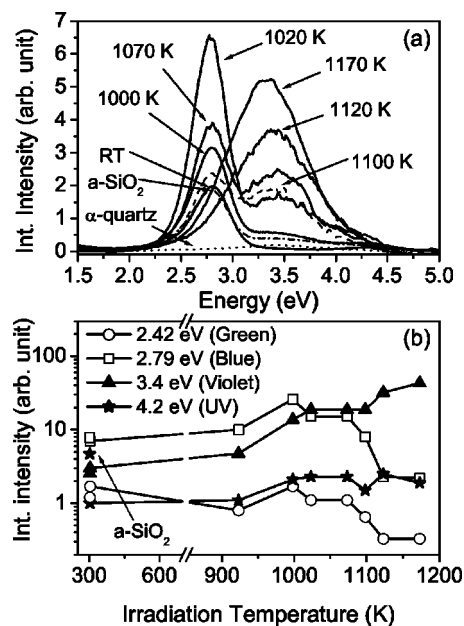


FIG. 2. (a) Cathodoluminescence spectra taken at RT in Ba-irradiated quartz at different implantation temperature between 300 and 1170 K. (b) Temperature dependence of the intensities of the extracted subpeaks.

of $E_A = 0.24 \pm 0.02$ eV, which is very close to the value obtained²¹ in the case of 50 keV Ne implantations in quartz (0.26 eV). This suggests similar defect annealing mechanisms in both cases and can be explained by the vacancy outdiffusion model.²¹

The room-temperature CL spectra shown in Fig. 2(a) were converted to the energy scale and decomposed into up to five Gaussian-shaped peaks (full width at half maximum ~ 0.3 – 0.7 eV) as described in Refs. 15 and 30. The CL emission intensities of all the subbands were corrected for the instrument response function, which was determined using a standard halogen calibration lamp. In Fig. 2(b), the integrated intensities of the four bands are plotted as a function of the sample temperature during the Ba implantations.

The nonimplanted sample, i.e., pure α -quartz, is characterized by a very weak and broad peak at 2 eV (620 nm) in the red region. The origin of this peak is due to electron irradiation induced defects in the SiO_2 matrix. This peak is attributed either to the nonbridging oxygen hole centers (NBOHC, $\text{O} \equiv \text{Si}-\text{O}$), or to the three coordinated silicon with a trapped electron ($\equiv \text{Si} \cdot$) or to the other associated precursors.^{15–17,19} The intensity of this weak band is insensitive to the presence of Ba ions and the implantation temperature and is therefore not shown in Fig. 2(b).

After Ba implantation at RT (and up to 1100 K) leading to amorphization, the CL spectrum showed peaks at 3.4 eV (363 nm, V =violet), 2.79 eV (442 nm, B =blue), 2.42 eV (510 nm, G =green), and at 4.2 eV (294 nm, UV). As illustrated in Fig. 2, all these peaks, except the violet one, were also observed in a quartz sample amorphized by 800 keV Ba^{++} -ion irradiation. As the projected range (260 nm) is larger compared to the electron penetration depth (~ 100 nm), CL arises only from the top amorphous SiO_2 layers. In particular, the peaks at 2.79 eV (B) and 4.2 eV (UV) are associated with oxygen deficiency centers (ODC, $\text{O} \equiv \text{Si}-\text{Si} \equiv \text{O}$) or with their precursors produced during irradiation.^{15–19} The blue one is the most dominant peak whose intensity reaches its maximum at 1020 K and which

almost disappears at 1120 K where complete SPEG is achieved [Fig. 1(a)]. The green peak at 2.42 eV may be connected to oxygen vacancy-interstitial pairs ($V_O(O_2C)i$), where V_O is the oxygen vacancy,^{14,18} or it may be due to irradiation-induced STE within the α -SiO₂ outgrowth at the top of the quartz crystal containing a large amount of peroxy linkages (Si–O–O–Si).¹⁵ Therefore, all these peaks are associated with various defect centers in the SiO₂ matrix.

In contrast to the CL bands from the SiO₂ matrix, the violet band at 3.4 eV (363 nm) grows in intensity with increasing sample temperature during irradiation and saturates above 1100 K, where complete SPEG occurs. The temperature-dependent CL exhibits this violet peak above 100 K and saturates at about 200 K. At this point it is interesting to note that the implanted Ba distribution [Fig. 1(a)] is independent of the implantation temperature. These facts suggest that the violet peak is associated with Ba-related defects in the SiO₂ network, such as $-O-Si-O-Ba^{2-}$. Also, it may be connected with the formation of Ba clusters or Ba colloids since Ba can capture oxygen from the silica network structure due its large electron affinity compared to Si.³ We noted that the energy of the violet peak changed slightly with the implantation temperature (3.34–3.50 eV) and that this peak has twice the width of the other peaks.

Finally, it is interesting to note that the UV peak at 4.2 eV has only been observed¹⁹ in the crystalline tetragonal stishovite phase or in amorphous SiO₂, but not in the hexagonal phase. Therefore, the disappearance of this peak above 1100 K indicates that the Ba-doped quartz has regained its hexagonal phase after the regrowth process. Therefore, the CL and RBS-C results clearly demonstrate that the luminescent properties of the dopant can be tuned by eliminating radiation-induced defect luminescence in the SiO₂ matrix via dynamic SPEG and this method is expected to work for doping α -quartz with other elements.

In conclusion, we have demonstrated that Ba can be incorporated via dynamic SPEG in single-crystalline α -quartz hardly affecting its crystalline structure. CL studies showed visible and UV peaks at 2.42, 2.79, 3.4, and 4.2 eV, all of which are associated with defect centers in the SiO₂ network. After achieving (almost) complete SPEG above 1100 K, these peaks either disappeared completely or decreased drastically in favor of a violet peak at 3.4 eV, which we tentatively connect to Ba-related optical centers in the SiO₂ network. These findings open up new possibilities to produce semiconductor or rare-earth or metallic small clusters and

nanostructures in α -quartz for fundamental studies and photonic applications.

The authors are thankful to Dr. M. Milosavljevic, D. Purschke, J. Zenneck, and L. Hamdi for extending their support for this work, which was funded by Deutsche Forschungsgemeinschaft.

- ¹P. J. Chandler, F. L. Lama, P. D. Townsend, and L. Zhang, *Appl. Phys. Lett.* **53**, 89 (1988).
- ²S. I. Najafi, *Introduction to Glass Integrated Optics* (Artech House, Boston, 1992).
- ³H. Hosono, *J. Non-Cryst. Solids* **187**, 457 (1995).
- ⁴E. K. Chang, M. Rohlfing, and S. G. Louie, *Phys. Rev. Lett.* **85**, 2613 (2000).
- ⁵T. Uchino, M. Takahashi, and T. Yoko, *Phys. Rev. Lett.* **86**, 1777 (2001).
- ⁶G. D. Mukherjee, S. N. Vaidya, and V. Sugandhi, *Phys. Rev. Lett.* **87**, 195501 (2001).
- ⁷A. Alderson and K. E. Evans, *Phys. Rev. Lett.* **89**, 225503 (2002).
- ⁸L. Rebohle, J. Von Borany, R. A. Yankov, W. Skorupa, I. E. Tyschenko, H. Förb, and K. Leo, *Appl. Phys. Lett.* **71**, 2809 (1997).
- ⁹Y. Q. Wang, G. L. Kong, W. D. Chen, H. W. Diao, C. Y. Chen, S. B. Zhang, and X. B. Liao, *Appl. Phys. Lett.* **81**, 4174 (2002).
- ¹⁰L. Rebohle, J. Von Borany, W. Skorupa, H. Förb, and S. Niedermeier, *Appl. Phys. Lett.* **77**, 969 (2000).
- ¹¹A. V. Kabashin and M. Meunier, *Appl. Phys. Lett.* **82**, 1619 (2003).
- ¹²H. Yang, X. Wang, H. Shi, S. Xie, F. Wang, X. Gu, and Xi Yao, *Appl. Phys. Lett.* **81**, 5144 (2002).
- ¹³K. S. Miu, K. V. Hchegolv, C. M. Yang, H. A. Atwater, M. L. Bongersma, and A. Polman, *Appl. Phys. Lett.* **68**, 2511 (1996).
- ¹⁴M. Yoshikawa, K. Matsuda, Y. Yamaguchi, T. Matsunobe, Y. Nagasawa, H. Fujino, and T. Yamane, *J. Appl. Phys.* **92**, 7153 (2002).
- ¹⁵M. A. S. Kalceff and M. R. Phillips, *Phys. Rev. B* **52**, 3122 (1995).
- ¹⁶H. S. Bae, T. G. Kim, C. N. Whang, S. Im, J. S. Yun, and J. H. Song, *J. Appl. Phys.* **91**, 4078 (2002).
- ¹⁷L. Skuja, B. Güttler, D. Schiel, and A. R. Silin, *Phys. Rev. B* **58**, 14296 (1998).
- ¹⁸M. A. Stevens-Kalceff, *Phys. Rev. Lett.* **84**, 3137 (2000).
- ¹⁹H. J. Fitting, T. Barfels, A. N. Trukhin, and B. Schmidt, *J. Non-Cryst. Solids* **279**, 51 (2001).
- ²⁰F. Harbsmeier and W. Bolse, *J. Appl. Phys.* **83**, 4049 (1998).
- ²¹S. Dhar, W. Bolse, and K. P. Lieb, *J. Appl. Phys.* **85**, 3120 (1999).
- ²²L. W. Hobbs, *J. Non-Cryst. Solids* **192/193**, 79 (1995).
- ²³K. P. Lieb, in *Encyclopedia on Nanoscience and Nanotechnology*, edited by H. S. Nalwa (American Scientific, Stevenson Ranch, CA, 2004).
- ²⁴F. Roccaforte, W. Bolse, and K. P. Lieb, *Appl. Phys. Lett.* **73**, 1349 (1998); *J. Appl. Phys.* **89**, 3611 (2001).
- ²⁵M. Gustafsson, F. Roccaforte, J. Keinonen, W. Bolse, L. Ziegeler, and K. P. Lieb, *Phys. Rev. B* **61**, 3327 (2000).
- ²⁶F. Roccaforte, S. Dhar, F. Harbsmeier, and K. P. Lieb, *Appl. Phys. Lett.* **75**, 2509 (1999).
- ²⁷F. Roccaforte, F. Harbsmeier, S. Dhar, and K. P. Lieb, *Appl. Phys. Lett.* **76**, 3709 (2000).
- ²⁸L. R. Doolittle, *Nucl. Instrum. Methods Phys. Res. B* **9**, 344 (1985).
- ²⁹J. F. Ziegler and J. P. Biersack, *Computer Program SRIM 2000*.
- ³⁰M. A. Stevens-Kalceff and M. R. Phillips, *Phys. Rev. B* **52**, 3122 (1995).